FTN multicarrier transmission based on tight Gabor frames

Alexandre Marquet, Damien Roque, Cyrille Siclet, Pierre Siohan

▶ **To cite this version:**

Alexandre Marquet, Damien Roque, Cyrille Siclet, Pierre Siohan. FTN multicarrier transmission based on tight Gabor frames. EURASIP Journal on Wireless Communications and Networking, 2017, 1, pp.97. ⟨10.1186/s13638-017-0878-3⟩. ⟨hal-01529661⟩

HAL Id: hal-01529661

https://hal.science/hal-01529661v1

Submitted on 31 May 2017

HAL is a multi-disciplinary open access archive for the deposit and dissemination of scientific research documents, whether they are published or not. The documents may come from teaching and research institutions in France or abroad, or from public or private research centers.

L'archive ouverte pluridisciplinaire **HAL**, est destinée au dépôt et à la diffusion de documents scientifiques de niveau recherche, publiés ou non, émanant des établissements d'enseignement et de recherche français ou étrangers, des laboratoires publics ou privés.

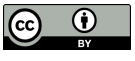

Distributed under a Creative Commons CC BY 4.0 - Attribution - International License

Marquet *et al. EURASIP Journal on Wireless Communications and Networking* (2017) 2017:97
DOI 10.1186/s13638-017-0878-3

EURASIP Journal on Wireless Communications and Networking

RESEARCH Open Access

FTN multicarrier transmission based on tight Gabor frames

Alexandre Marquet[1,2*], Damien Roque[2], Cyrille Siclet[1] and Pierre Siohan[3]

Abstract

A multicarrier signal can be synthesized thanks to a symbol sequence and a Gabor family (i.e., a regularly time–frequency shifted version of a generator pulse). In this article, we consider the case where the signaling density is increased such that inter-pulse interference is unavoidable.
Over an additive white Gaussian noise channel, we show that the signal-to-interference-plus-noise ratio is maximized when the transmitter and the receiver use the same tight Gabor frame. What is more, we give practical efficient realization schemes and show how to build tight frames based on usual generators. Theoretical and simulated bit-error probability are given for a non-coded system using quadrature amplitude modulations. Such a characterization is then used to predict the convergence of a coded system using low-density parity-check codes. We also study the robustness of such a system to errors on the received bits in an interference cancellation context.

Keywords: Multicarrier modulations, Faster-than-Nyquist signaling, Linear system, Optimal pulse shapes, Gabor frames, Interference analysis, Interference cancellation, Low-density parity-check codes

1 Introduction

In most of current communication systems, information symbols can be transmitted and reconstructed thanks to linear operations. More precisely, the synthesis and analysis families used in the transmitter and the receiver form biorthogonal frames (also known as Riesz bases). In a single-carrier band-limited scenario, this requires the Nyquist criterion to be respected [1]. In other words, the transmission rate must be lower than the bilateral bandwidth of the transmitted signal.

With an increasing need of spectral efficiency driven by overcrowded frequency bands, the main strategy relies on an increase of constellation size while keeping a constant transmission power, bandwidth, and symbol rate (below the Nyquist limit). This choice induces a decrease of the minimum Euclidean distance between symbols, and the transmitted signal becomes more sensitive to noise, thus increasing bit-error probability [2].

A more unusual way to improve spectral efficiency is to increase the symbol rate until the Nyquist criterion is overridden, leading to unavoidable inter-pulse interference (IPI). This idea has been proposed by J. Mazo under the denomination "*faster-than-Nyquist*" (FTN) [3]. His work showed that up to a certain point, an increase of the Nyquist symbol rate keeps the minimal distance between symbols unchanged. As a consequence, considering the work of G.D. Forney on the optimal detection in presence of inter-symbol interference, one can achieve identical bit-error probability using an optimal receiver [2].

FTN transmission techniques can be extended to multicarrier modulations [4]. In this case, denoting F_0 the inter-carrier spacing and T_0 the multicarrier symbol duration, it can be shown that if $\rho = 1/(F_0 T_0) > 1$, then the synthesis and analysis families, respectively used for transmission and reception, can no longer be biorthogonal but can still form overcomplete frames [5–7]. This leads to IPI both in time and/or frequency. Numerous studies focus on the realization of coded multicarrier FTN systems using, in particular, series or parallel concatenations [8] as well as turbo equalization techniques [9]. Studies of these latter systems over additive white Gaussian noise (AWGN) channels show great performance, confirming their relevance, even if their intrinsic complexity makes their design

*Correspondence: alexandre.marquet@gipsa-lab.grenoble-inp.fr
[1]Univ. Grenoble Alpes, GIPSA-Lab, F-38400 Grenoble, France
[2]Institut Supérieur de l'Aéronautique et de l'Espace (ISAE-SUPAERO), Univ. Toulouse, F-31055 Toulouse, France
Full list of author information is available at the end of the article

Springer Open

© The Author(s). 2017 **Open Access** This article is distributed under the terms of the Creative Commons Attribution 4.0 International License (http://creativecommons.org/licenses/by/4.0/), which permits unrestricted use, distribution, and reproduction in any medium, provided you give appropriate credit to the original author(s) and the source, provide a link to the Creative Commons license, and indicate if changes were made.

and performance comparison particularly demanding in terms of simulation time.

In this article, we study a linear multicarrier system operating with overcomplete Gabor frames (i.e., a generalization of an FTN system), as it plays a fundamental role in more complex systems (e.g., decision feedback equalizers, forward error correction, turbo equalizers). Our work includes guidelines for the design of optimal transmission and reception Gabor frames with respect to the signal-to-interference-plus-noise ratio (SINR) criterion over an AWGN channel. An efficient realization scheme is proposed and assessed with several classical pulse shapes (i.e., square-root-raised-cosine, rectangular...) built using the Wexler–Raz theorem.

This article is constructed as follows. Section 2 establishes input–output relations of the system in presence of noise, based on frame theory. This theoretical framework enables a closed-form expression of the SINR and the theoretical bit-error probability (BEP), assuming a circularly symmetric Gaussian distribution of the interference term. We then give in Section 3 practical efficient realization schemes. Next, Section 4 shows how we can easily find pulse shapes generating dual and tight frames. Section 5 first focuses on the statistical properties of the interference in an empirical way, as to confirm the relevance of its Gaussian approximation. We then present bit-error rate (BER) simulations to verify our theoretical results. In particular, we show how our closed-form BEP expression can predict the performance of a coded system. The last simulation scenario analyzes the relevance of interference cancellation techniques in this communication context. Finally, conclusions and insights are presented in Section 6.

Notations are described in the following. Sets are denoted by uppercase roman bold letters, with $\mathbf{Z}$, $\mathbf{R}$ and $\mathbf{C}$ defined as the sets of integers, real numbers and complex numbers, respectively. Lowercase bold letters denote families of vectors. The linear span and the closed linear span of any family of vectors $\boldsymbol{x}$ are denoted $\mathrm{Span}(\boldsymbol{x})$ and $\overline{\mathrm{Span}}(\boldsymbol{x})$, respectively. The conjugation operator is denoted $(\cdot)^*$, and the expectation operation is given by $\mathrm{E}(\cdot)$. The complex-circular normal distribution, with mean m and variance σ^2 is written $\mathcal{CN}(m,\sigma^2)$. Let $x \in \mathbf{R}$, we denote $\lfloor x \rfloor$ the greatest integer such that $\lfloor x \rfloor \leq x$, and $\lceil x \rceil$ the least integer such that $\lceil x \rceil \geq x$. For any continuous time signal $x(t)$, $t \in \mathbf{R}$ and discrete-time signal $y[k]$, $k \in \mathbf{I} \subset \mathbf{Z}$, we define the spaces $\mathcal{L}_2(\mathbf{R}) = \{x : \mathbf{R} \to \mathbf{C} / \int_{-\infty}^{+\infty} |x(t)|^2 \,\mathrm{d}t < +\infty\}$ and $\ell_2(\mathbf{I}) = \{y : \mathbf{I} \to \mathbf{C} / \sum_{k\in\mathbf{I}} |y[k]|^2 < +\infty\}$. Let us now define $x_1(t), x_2(t) \in \mathcal{L}_2(\mathbf{R})$, such that the $\mathcal{L}_2$-inner product of those two signals is given by

$$\langle x_1, x_2 \rangle = \int_{-\infty}^{+\infty} x_1^*(t) x_2(t) \,\mathrm{d}t \tag{1}$$

and the $\mathcal{L}_2$-norm of $x_1(t)$ is given by $\|x_1\| = \sqrt{\langle x_1, x_1 \rangle}$. The ℓ_2-inner product and its induced norm is defined similarly in the case of discrete-time signals.

2 System model

2.1 Input–output relations in presence of white Gaussian noise

Let us denote $\boldsymbol{c} = \{c_{m,n}\}_{(m,n)\in\boldsymbol{\Lambda}} \in \ell_2(\boldsymbol{\Lambda})$ with $\boldsymbol{\Lambda} \subset \mathbf{Z}^2$, a sequence of zero-mean, independent, and identically distributed (i.i.d.) coefficients. Its variance is σ_c^2. The multicarrier equivalent baseband signal is given by:

$$s(t) = \sum_{(m,n)\in\boldsymbol{\Lambda}} c_{m,n} g_{m,n}(t), \quad t \in \mathbf{R}, \tag{2}$$

where $\boldsymbol{g} = \{g_{m,n}\}_{(m,n)\in\boldsymbol{\Lambda}}$ is a synthesis Gabor family, with parameters $F_0, T_0 > 0$ and whose elements are given by the generator $g(t) \in \mathcal{L}_2(\mathbf{R})$ such that:

$$g_{m,n}(t) = g(t - nT_0) e^{j2\pi m F_0 t}, \quad (m,n) \in \boldsymbol{\Lambda}. \tag{3}$$

As a result, the information carried by $\boldsymbol{c}$ is regularly spread in the time–frequency plane (Fig. 1) with a minimum distance F_0 in frequency and T_0 in time.

In a real case scenario, transmission is bounded in time and in frequency such that $\boldsymbol{\Lambda} = \{0,\dots,M-1\} \times \{0,\dots,K-1\}$ where M, K are strictly positive integers representing respectively the number of subcarriers and the number of multicarrier symbols to be transmitted. Such a restriction to a finite signaling set induces the convergence of the sum in (2). Nevertheless, it can still contain a large amount of terms, so it is important to make it BIBO (bounded-input bounded-output) stable. In other words, $s(t)$ defined in Eq. (2) should be well defined even if $\boldsymbol{\Lambda} = \mathbf{Z}^2$. Denoting $\mathcal{H}_{\boldsymbol{g}} = \overline{\mathrm{Span}}(\boldsymbol{g})$, the stability of (2) is

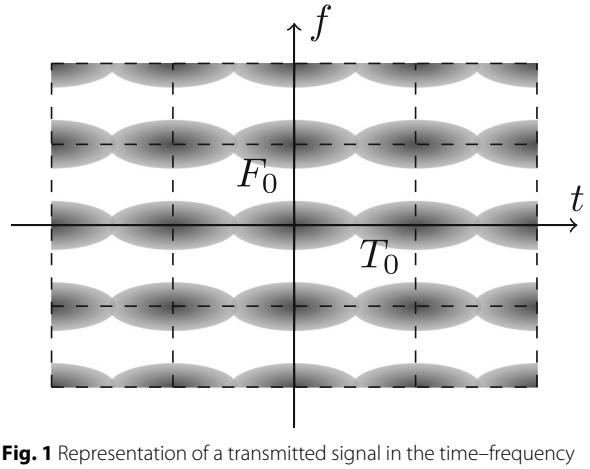

Fig. 1 Representation of a transmitted signal in the time–frequency plane. Here, the parameters g, F_0 and T_0 are chosen such that pulse shapes do not overlap in the frequency domain

guaranteed when $\boldsymbol{g}$ is a Bessel sequence, which means that we can find an upper bound $B_g > 0$ such as:

$$\sum_{(m,n)\in\boldsymbol{\Lambda}} \left|\langle g_{m,n}, x\rangle\right|^2 \leq B_g \|x\|^2, \quad x \in \mathcal{H}_{\boldsymbol{g}}, \tag{4}$$

In order to retrieve the data $\boldsymbol{c}$ from the knowledge of $s(t)$, it is furthermore necessary and sufficient for $\boldsymbol{g}$ to be a linearly independent family. Hence, $\boldsymbol{g}$ should be a Riesz basis for $\mathcal{H}_{\boldsymbol{g}}$, in other words a linearly independent family for which we can find $0 < A_g \leq B_g$ such that:

$$A_g \|x\|^2 \leq \sum_{(m,n)\in\boldsymbol{\Lambda}} \left|\langle g_{m,n}, x\rangle\right|^2 \leq B_g \|x\|^2, \quad x \in \mathcal{H}_{\boldsymbol{g}}. \tag{5}$$

If one defines the density of the Gabor frame $\boldsymbol{g}$ as $\rho = 1/(F_0 T_0)$, the former linear independence condition requires $\rho \leq 1$. In this context, there exists an analysis Gabor family $\boldsymbol{h}$ such that

$$c_{p,q} = \langle h_{p,q}, s\rangle, \quad (p,q) \in \boldsymbol{\Lambda}. \tag{6}$$

On the contrary, in order to increase the spectral efficiency of the system (for a fixed number of bits per symbol), this article focuses on the case where $\rho > 1$. Thus, this increase in spectral efficiency is counterbalanced by an induced interference. Indeed, when $\rho > 1$, $\boldsymbol{g}$ is necessarily a linearly dependent Gabor family, but it may be an overcomplete frame of $\mathcal{L}_2(\mathbf{R})$, i.e., a family for which (5) is valid not only for $x \in \mathcal{H}_{\boldsymbol{g}}$ but also for every $x \in \mathcal{L}_2(\mathbf{R})$. In this case, (2) is always stable and $\mathcal{H}_{\boldsymbol{g}} = \mathcal{L}_2(\mathbf{R})$. However, $\boldsymbol{g}$ cannot be a basis of $\mathcal{L}_2(\mathbf{R})$.

A linear receiver is considered as a first stage of a more complete FTN system (necessarily non-linear in order to yield acceptable performance). In this context, the estimated symbols $\hat{\boldsymbol{c}} = \{\hat{c}_{p,q}\}_{(p,q)\in\boldsymbol{\Lambda}}$ are given by

$$\hat{c}_{p,q} = \langle \check{g}_{p,q}, r\rangle, \quad (p,q) \in \boldsymbol{\Lambda}, \tag{7}$$

where $\check{\boldsymbol{g}} = \{\check{g}_{m,n}\}_{(m,n)\in\boldsymbol{\Lambda}}$ is an analysis Gabor family, $r(t) = s(t) + n(t)$ is the signal seen by the receiver where $n(t)$ is a zero-mean circularly symmetric Gaussian noise, independent from the symbols, and whose bilateral power spectral density is $\gamma_n(f) = 2N_0, f \in \mathbf{R}$.

2.2 Interference and noise terms analysis

By rewriting (7) thanks to (2) and using the linearity of the inner product, we obtain:

$$\hat{c}_{p,q} = \underbrace{c_{p,q}\langle \check{g}_{p,q}, g_{p,q}\rangle}_{\tilde{c}_{p,q}:\text{useful signal}} + \underbrace{\sum_{(m,n)\in\boldsymbol{\Lambda}\setminus\{(p,q)\}} c_{m,n}\langle \check{g}_{p,q}, g_{m,n}\rangle}_{i_{p,q}:\text{interference}} + \underbrace{\langle \check{g}_{p,q}, n\rangle}_{n_{p,q}:\text{noise}}. \tag{8}$$

We have suggested in [10] that the SINR shoud be maximized when $\check{\boldsymbol{g}}$ and $\boldsymbol{g}$ are dual canonical (i.e., $A_g = 1/A_{\check{g}}$ and $B_g = 1/B_{\check{g}}$) tight (i.e., $A_g = B_g$ and $\check{\boldsymbol{g}} = \boldsymbol{g}/A_g$) frames. This enables an analytic expression for the SINR. Indeed, let us denote $\sigma^2_{\tilde{c}_{p,q}}$, $\sigma^2_{i_{p,q}}$ and $\sigma^2_{n_{p,q}}$ the variances of the useful signal, the interference, and filtered noise, respectively. Then, the SINR at frequency index p and time index q is given by:

$$\mathrm{SINR}_{p,q} = \frac{\sigma^2_{\tilde{c}_{p,q}}}{\sigma^2_{i_{p,q}} + \sigma^2_{n_{p,q}}}. \tag{9}$$

Since we assume that $c_{p,q}$ is zero-mean with variance σ_c^2, we deduce from (8) that $\tilde{c}_{p,q}$ is zero-mean too with variance $\sigma^2_{\tilde{c}_{p,q}} = \sigma_c^2 \left|\langle \check{g}_{p,q}, g_{p,q}\rangle\right|^2$. What is more, we impose that $\check{\boldsymbol{g}} = \boldsymbol{g}/A_g$, and therefore,

$$\left|\langle \check{g}_{p,q}, g_{p,q}\rangle\right|^2 = \left|\langle g_{p,q}, g_{p,q}\rangle\right|^2 / A_g^2 = \|g_{p,q}\|^4 / A_g^2 = \|g\|^4 / A_g^2, \tag{10}$$

using (3). In addition, since $\boldsymbol{g}$ is assumed to be a tight frame, $\|g\|^2 = A_g/\rho$ [11]. Thus, finally,

$$\left|\langle \check{g}_{p,q}, g_{p,q}\rangle\right|^2 = 1/\rho^2, \tag{11}$$

so that $\sigma^2_{\tilde{c}_{p,q}}$ is independent from p and q and

$$\sigma^2_{\tilde{c}_{p,q}} = \sigma^2_{\tilde{c}} = \sigma_c^2/\rho^2. \tag{12}$$

As for the interference term $i_{p,q}$, using the fact that symbols $c_{m,n}$ are assumed to be zero-mean, i.i.d. and with variance σ_c^2, (8) shows that $i_{p,q}$ is zero-mean too with variance given by

$$\sigma^2_{i_{p,q}} = \mathrm{E}\left(|i_{p,q}|^2\right) = \sigma_c^2 \left(\sum_{(m,n)\in\boldsymbol{\Lambda}} \left|\langle \check{g}_{p,q}, g_{m,n}\rangle\right|^2 - \left|\langle \check{g}_{p,q}, g_{p,q}\rangle\right|^2 \right). \tag{13}$$

Since we impose that $\boldsymbol{g}$ is a tight frame with bound A_g and $\check{\boldsymbol{g}} = \boldsymbol{g}/A_g$, we obtain that $\check{\boldsymbol{g}}$ is also a tight frame with bound $1/A_g$. Thus, by definition:

$$\sum_{(m,n)\in\Lambda} \left|\langle \check{g}_{p,q}, g_{m,n}\rangle\right|^2 = \|g_{p,q}\|^2 / A_g = 1/\rho. \tag{14}$$

Then, combining Eqs. (11), (13), and (14), we obtain

$$\sigma^2_{i_{p,q}} = \sigma_i^2 = \sigma_c^2(\rho - 1)/\rho^2. \tag{15}$$

Concerning the filtered noise $n_{p,q}$, (8) shows that it is Gaussian, zero-mean with variance

$$\sigma^2_{n_{p,q}} = \mathrm{E}\left(|n_{p,q}|^2\right) = 2N_0 \|\check{g}_{p,q}\|^2 = \frac{2N_0}{\rho A_g} = \sigma_n^2, \tag{16}$$

Finally, let us denote $E_s = \frac{1}{2}\sigma_c^2 \|g\|^2$ the per symbol energy. Recalling $\|g\|^2 = A_g/\rho$, we get

$$E_s = \frac{\sigma_c^2 A_g}{2\rho}. \tag{17}$$

And finally, combining Eqs. (12), (15), (16), and (17), we obtain that the SINR is independent from the frequency and time indices and expressed by:

$$\mathrm{SINR}_{p,q} = \mathrm{SINR} = \frac{1}{\rho - 1 + \frac{N_0}{E_s}}. \tag{18}$$

We can see that the interference term $i_{p,q}$ is a random variable independent from the noise and corresponding to the sum of a large number of random variables $\tilde{c}_{m,n}$ which are zero-mean, independent, and following the same type of law but with different variances $\sigma^2_{\tilde{c}_{m,n}}$:

$$\tilde{c}_{m,n} = c_{m,n}\langle \check{g}_{p,q}, g_{m,n}\rangle \text{ and } \sigma^2_{\tilde{c}_{m,n}} = \sigma_c^2 |\langle \check{g}, g_{m-p,n-q}\rangle|^2. \tag{19}$$

All the conditions for applying the central limit theorem are thus not fulfilled, but as shown by our simulations in Section 5.1, the Gaussian approximation is accurate for the sake of error–probability estimation. That is why in the following, we will assume $i_{p,q} \sim \mathcal{CN}(0, \sigma_i^2)$ independent from the noise. This is analogous to a case where the symbols would have been transmitted through an AWGN channel characterized by a signal-to-noise ratio (SNR) given by (18). It is interesting to note that the noise term $n_{p,q}$ is a colored zero-mean random variable following a Gaussian distribution.

2.3 Theoretical error probability with a linear *M*-ary system

We now restrict our analysis to the case where the symbols $\boldsymbol{c}$ are taken from an P-ary constellation, such as quadrature amplitude modulation (P-QAM) or phase-shift keying (P-PSK) with P the size of the constellation.

Approximating the interference distribution with a normal distribution, let us use classical formulas for BER in presence of AWGN [12, 13]. Given that these classical formulas usually give BER as a function of E_b/N_0 (with $E_b = E_s/\log_2(\mathrm{P})$ the per-bit energy), the only adaptation to be made in order to take into account the intereference is to change E_b/N_0 to $\mathrm{SINR}/\log_2(\mathrm{P})$.

We give two examples, using the two constellations that will be used throughout this paper. First, for a classical (orthogonal) system using Gray code bit mapping with quadrature phase-shift keying (or 4-QAM) over AWGN, the BER is given by $Q(2E_b/N_0)$. Thus, the BER for a multicarrier FTN system using tight frames in the same scenario is given by:

$$P_{e,\mathrm{QPSK}} = Q\left(\sqrt{\mathrm{SINR}}\right) = Q\left(\sqrt{\frac{1}{(\rho-1) + \frac{N_0}{2E_b}}}\right). \tag{20}$$

Using identical reasoning on the results from [13], changing the constellation to 16-QAM gives the following bit-error probability:

$$P_{e,16\mathrm{QAM}} = \frac{1}{4}\sum_{k=1}^{2}\sum_{i=0}^{\left(1-2^{-k}4\right)-1}(-1)^{\left\lfloor i2^{k-3}\right\rfloor}\left(2^{k-1} - \left\lfloor i2^{k-3} + \frac{1}{2}\right\rfloor\right) \cdot Q\left((2i+1)\sqrt{\frac{\mathrm{SINR}}{5}}\right). \tag{21}$$

3 Discrete-time implementation of the linear system

In this section, we derive a discrete-time efficient implementation of the linear multicarrier system. Surprinsingly, such a process does not seem well documented in the literature. In the following, we first derive the input-output relation of a causal discrete-time system. Then, we develop an efficient time-domain implementation using the fast Fourier transform algorithm and finite impulse response filtering.

3.1 Discrete-time equivalent linear system

Let us recall the multicarrier transceiver defined by (2) and (7) with a finite number of subcarriers M and a finite number of multicarrier symbols K, such that $\boldsymbol{\Lambda} = \{0,\ldots,M-1\} \times \{0,\ldots,K-1\}$. The transmission generator $g(t)$ is supposed to have a bandwidth W_g. It results an overall system bandwidth $W = (M-1)F_0 + W_g$ that can be approximated by MF_0 hereafter assuming $|W_g - F_0|/(MF_0) \ll 1$. In practice, it is generally the case if we consider a large number of subcarriers. As a consequence, the signal can be sampled at critical rate $1/T_s = MF_0$ and we denote N the number of samples per multicarrier symbol such that $T_0 = NT_s$. Note that the density can be rewritten as $\rho = M/N$, and considering a unique multicarrier symbol, the FTN case is illustrated in the discrete-time domain by a number of samples per multicarrier symbol N less than the number of subcarriers M.

In order to yield a causal transceiver with finite impulse response generators, the impulse response $g(t)$ and $\check{g}(t)$ are truncated, and we define three positive integer parameters D, L_g, and $L_{\check{g}}$ such that $g(t)$ and $\check{g}^H(t) = \check{g}^*(-t)$ have their support included in $[-((D+1)/2)T_s; (L_g-(D+1)/2)T_s[$ and $[-((D+1)/2)T_s; (L_{\check{g}}-(D+1)/2)T_s[$, respectively. Therefore, the discrete-time causal generators can be expressed as

$$g[k] = \sqrt{T_s}g\left(\left(k - \frac{D}{2}\right)T_s\right), \tag{22}$$

$$\check{g}[k] = \sqrt{T_s}\check{g}\left(\left(k - \frac{D}{2}\right)T_s\right), \tag{23}$$

where the factor $\sqrt{T_s}$ is used for energy normalization. From (2), the discrete-time transmitted signal can be expressed as

$$s[k] = \sqrt{T_s} s\left(\left(k - \frac{D}{2}\right) T_s\right) = \sum_{(m,n)\in\mathbf{\Lambda}} c_{m,n} g_{m,n}[k]\,, \tag{24}$$

with

$$g_{m,n}[k] = \sqrt{T_s} g_{m,n}\left(\left(k - \frac{D}{2}\right) T_s\right) \tag{25}$$

$$= g[k - nN]\, e^{j2\pi \frac{m}{M}\left(k - \frac{D}{2}\right)}. \tag{26}$$

Assuming an ideal channel (*i.e.*, $r[k] = s[k]$), an estimated symbol $\tilde{c}_{p,q}$ for all $(p,q) \in \Lambda$ can be obtained in a similar way as (7):

$$\tilde{c}_{p,q} = \langle \check{g}_{p,q}, r \rangle = \sum_{k=-\infty}^{+\infty} \check{g}^*_{p,q}[k]\, r[k]\,, \tag{27}$$

with

$$\check{g}_{p,q}[k] = \sqrt{T_s} \check{g}_{p,q}\left(\left(k - \frac{D}{2}\right) T_s\right) \tag{28}$$

$$= \check{g}[k - qN]\, e^{j2\pi \frac{p}{M}\left(k - \frac{D}{2}\right)}. \tag{29}$$

Notice that the support of $g[k]$ and $\check{g}[k]$ are $\{0, \ldots, L_g - 1\}$ and $\{D - (L_{\check{g}} - 1), D\}$, respectively. In order to ensure a causal receiver, we define $d = \lceil D/N \rceil$ and consider the $(q-d)$th estimated multicarrier symbol:

$$\tilde{c}_{p,q-d} = \sum_{k=-\infty}^{+\infty} \check{g}[k - qN + dN]\, e^{-j2\pi \frac{m}{M}\left(k - \frac{D}{2}\right)} r[k]\,. \tag{30}$$

Given (22) and (23), it is usually desirable to use short-length generators in order to keep a low latency transceiver. In the following, for the sake of clarity, causality of the transceiver will be implicit.

Input:

M: number of carriers (integer)
N: number of samples per multicarrier symbol (integer)
K: number of multicarrier symbol (integer)
$\boldsymbol{c}$: multicarrier symbols (matrix of size $M \times K$)
$\boldsymbol{g}$: generator (array of size L_g)
D: delay applied to g to guarantee causality (integer)

Output:

$\boldsymbol{s}$: modulated signal (array of size $L_s = (K-1)N + L_g$)

for $0 \le n \le K-1$ **do** ▷ Rotation
  for $0 \le m \le M-1$ **do**
    $c'[m][n] \leftarrow c[m][n] \times \exp\left(-j \times \pi \times \frac{m}{M} \times D\right)$
  end for
end for

$\boldsymbol{C} \leftarrow \mathrm{IFFT}(\boldsymbol{c'})$ ▷ Inverse discrete Fourier transform

for $0 \le k \le L_s - 1$ **do** ▷ Filtering
  $n_1 \leftarrow \max\left(0, \left\lceil \frac{k+1-L_g}{N} \right\rceil\right)$
  $n_2 \leftarrow \min\left(\left\lfloor \frac{k}{N} \right\rfloor, K-1\right)$
  for $n_1 \le n \le n_2$ **do**
    $s[k] \leftarrow s[k] + C[k - M \times \lfloor k/M \rfloor][n] \times g(k - n \times N)$
  end for
end for

Fig. 2 Multicarrier transmitter algorithm

Input:

M: number of carriers (integer)

N: number of samples per multicarrier symbol (integer)

K: number of multicarrier symbol (integer)

$\boldsymbol{r}$: received modulated signal (array of size $L_r = M \times K$)

$\check{\boldsymbol{g}}$: generator (array of size $L_{\check{g}}$)

D: delay applied to $\check{g}$ to guarantee causality (integer)

Output:

$\tilde{\boldsymbol{c}}$: estimated symbols (array of size $M \times K$)

for $0 \leq p \leq M-1$ **do** ▷ Filtering

  for $0 \leq q \leq K-1$ **do**

    $l_1 \leftarrow \max\left(0, \left\lceil \frac{q \times N - p}{M} \right\rceil\right)$

    $l_2 \leftarrow \min\left(\left\lfloor \frac{L_{\check{g}} - 1 - p + q \times N}{M} \right\rfloor, \left\lfloor \frac{L_r - 1 - p}{M} \right\rfloor\right)$

    for $l_1 \leq l \leq l_2$ **do**

      $\tilde{C}'[p][q] \leftarrow \tilde{C}'[p][q] + r[k + l \times M] \times \check{g}[k + l \times M - q \times N]$

    end for

  end for

end for

$\tilde{\boldsymbol{c}}' \leftarrow \mathrm{FFT}(\tilde{\boldsymbol{C}}')$ ▷ Discrete Fourier transform

for $0 \leq p \leq M-1$ **do** ▷ Inverse rotation

  for $0 \leq q \leq K-1$ **do**

    $\tilde{c}[p][q] = \tilde{c}'[p][q] \times \exp\left(-j \times \pi \times \frac{p}{M} \times D\right)$

  end for

end for

Fig. 3 Multicarrier receiver algorithm

3.2 Time domain efficient implementation of the linear system

A detailed algorithmic description of the linear transmitter/receiver is proposed in Figs. 2 and 3. Even if the transceiver is designed for the FTN case, it remains generic enough to comply with any density ($0 < \rho < +\infty$) and arbitrary generator lengths $L_g \geq N$ and $L_{\check{g}} \geq N$. However, further simplifications should be done in various particular cases (e.g., short filters, rectangular filters) [14]. The transmitter's and the receiver's algorithms can be divided into three steps described below: rotation, discrete Fourier transform, and filtering.

Symbol rotation is performed at the transmitter and at the receiver side in order to account for the delay D required to yield a causal transceiver. Since such operations are dual and have no consequence on the performance of the system, they can be omitted at both ends for simulation purpose.

The discrete Fourier transform step should be implemented, thanks to the FFT algorithm, in order to ensure a computational complexity $O(M \log M)$. In Figs. 2 and 3, operations denoted FFT and its inverse (IFFT) refer to a column-wise implementation of [15]. Interestingly, but without computational complexity gain, rotations and discrete Fourier transform operations can be merged together with the help of the chirp-z transform, as proposed in [16].

The filtering step takes into account the length of the signals (i.e., L_s, L_r, L_g, $L_{\check{g}}$) as well as the parameters M and N to avoid unnecessary operations (e.g., multiplications by zero). For example, at the transmitter side, the summation bounds over n in (24) can be restricted to $n_1[k]$ and $n_2[k]$, respectively, as illustrated by Fig. 4. A similar restriction holds at the receiver side. Lastly, a circuit implementation can further simplify the filtering step if pulse shaping operations are performed thanks to polyphase filtering. Such a hardware implementation is beyond the scope of

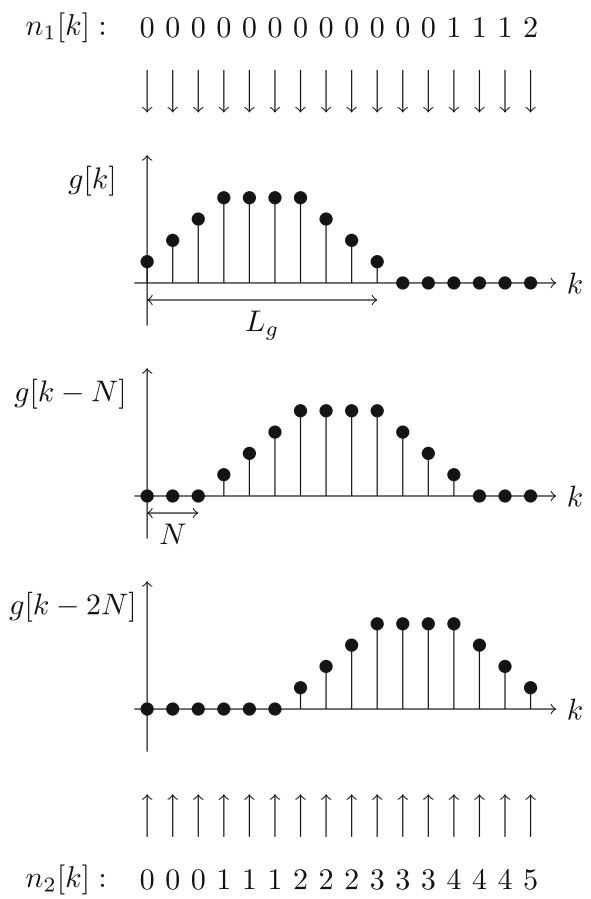

Fig. 4 Illustration of the summation bound restriction at the filtering stage of the transmitter. The following parameters are taken: $L_g = 10, N = 3, K = 3$

this article; however, the reader will find realizations in [17–19].

4 Selection of the generators

We have seen in Section 2.1 that a Gabor family $\boldsymbol{g}$ may be a Riesz basis of $\overline{\text{Span}}(\boldsymbol{g})$ if $\rho \leq 1$ or a frame of $\mathcal{L}_2(\mathbf{R})$ if $\rho > 1$. The case $\rho \leq 1$ corresponds to "slower-than-Nyquist" (STN) or Nyquist rate ($\rho = 1$) systems, and it is the only possibility to obtain a perfect reconstruction (PR) system. On the contrary, Gabor families with $\rho > 1$ constitute FTN multicarrier systems. The PR case ($\rho \leq 1$) has been well studied and is also often referred to as filtered multitone (FMT) systems [20], or oversampled orthogonal (or biorthogonal) frequency-division multiplexing (OFDM and BFDM) systems [21]. Such systems are also said to be orthogonal when the same generator is used at transmission and reception and biorthogonal if otherwise.

Classically, authors simply use filters generating orthogonal systems at the Nyquist rate (or below the Nyquist rate) and then reduce the time interval [4, 9] with a normalization factor. Thus, given a PR (STN or Nyquist rate) system, with generator $\tilde{g}$ and frequency and time spacings $\tilde{F}_0$ and $\tilde{T}_0$, respectively, a common and classical way to get an FTN system is to use a generator $g = \alpha\tilde{g}$ ($\alpha \in \mathbf{R}$) and frequency and time spacings $F_0 = \tilde{F}_0$ and $T_0 = 1/(\rho F_0) < \tilde{T}_0$, respectively. However, this does not guarantee that the obtained system is based on tight frames. On the contrary, here, we want to use filters generating tight Gabor frames, ensuring a maximal SINR. To this extent, we can take advantage of the strong link between systems with $\rho > 1$ and $\rho < 1$. Indeed , the Wexler–Raz theorem ([5], Theorem 9.3.4) states that if $\tilde{\boldsymbol{g}}$ and $\tilde{\check{\boldsymbol{g}}}$ yield a PR (bi)orthogonal system , then $\boldsymbol{g}$ and $\check{\boldsymbol{g}}$ are two dual frames when:

$$\tilde{F}_0 = \frac{1}{T_0}, \quad \tilde{T}_0 = \frac{1}{F_0}, \quad \tilde{g} = \frac{1}{\sqrt{F_0 T_0}}\, g, \quad \tilde{\check{g}} = \frac{1}{\sqrt{F_0 T_0}}\, \check{g}. \tag{31}$$

And, finally, taking $\tilde{g} = \tilde{\check{g}}$, let us obtain tight frames with $A_g = 1$. A summary of duality relations between PR-FMT systems (biorthognal) and FTN-FMT systems can be found in Table 1.

There are various ways to get PR-FMT filters. The more obvious one is to simply use at transmission and reception the same rectangular filter $\tilde{g}(t) = \tilde{\check{g}}(t) = \sqrt{\tilde{F}_0}\Pi(\tilde{F}_0 t) = \tilde{F}_0$ if $|t| < 1/(2\tilde{F}_0)$ and $\tilde{g}(t) = \tilde{\check{g}}(t) = 0$ if $|t| > 1/(2\tilde{F}_0)$. This leads to an orthogonal

Table 1 Duality relations between STN and FTN multicarrier communication

System	STN	FTN
Frequency spacing	$\tilde{F}_0 = 1/T_0$	$F_0 = 1/\tilde{T}_0$
Time spacing	$\tilde{T}_0 = 1/F_0$	$T_0 = 1/\tilde{F}_0$
Density	$\tilde{\rho} = 1/(\tilde{F}_0\tilde{T}_0) = F_0 T_0 < 1$	$\rho = 1/(F_0 T_0) = \tilde{F}_0\tilde{T}_0 > 1$
Interference mitigation	PR with biorthogonal frames	Dual frames
Noise reduction	PR with orthogonal frames	Tight frames with $A_g = 1$
Transmission generator	$\tilde{g} = g/\sqrt{\tilde{\rho}} = \sqrt{\rho}\, g$	$g = \tilde{g}/\sqrt{\rho} = \sqrt{\tilde{\rho}}\, \tilde{g}$
Reception generator	$\tilde{\check{g}} = \check{g}/\sqrt{\tilde{\rho}} = \sqrt{\rho}\, \check{g}$	$\check{g} = \tilde{\check{g}}/\sqrt{\rho} = \sqrt{\tilde{\rho}}\, \tilde{\check{g}}$

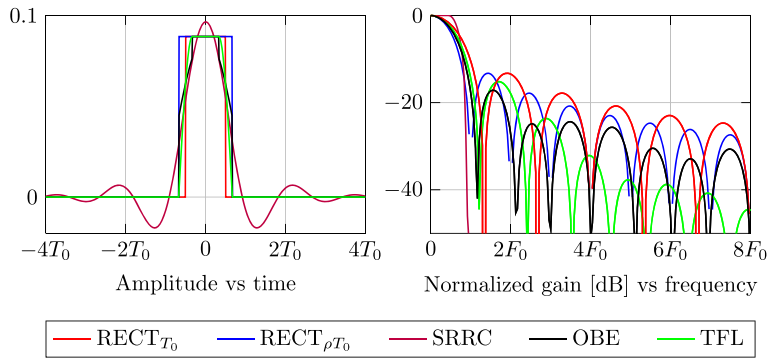

Fig. 5 Generator filters providing dual or tight frames for $\rho = 4/3$

PR-FMT system. By duality, choosing $g(t) = \check{g}(t) = 1/\sqrt{\rho T_0}\Pi(t/T_0)$ leads to tight frames. This will be referred as the RECT_{T_0} generator in the rest of this text.

Setting $\tilde{g}(t) = \sqrt{\tilde{F}_0}\Pi(\tilde{F}_0 t)$ and $\check{\tilde{g}}(t) = \sqrt{\tilde{F}_0}\Pi(t/\tilde{T}_0)$ leads to a PR biorthogonal STN system, but it is not orthogonal since $\tilde{g} \neq \check{\tilde{g}}$. By duality, this allows us to obtain dual frames which are not tight: $g(t) = 1/\sqrt{\rho T_0}\Pi(t/T_0) = \mathrm{RECT}_{T_0}(t)$ and $\check{g}(t) = 1/\sqrt{\rho T_0}\Pi(t/\rho T_0)) = \mathrm{RECT}_{\rho T_0}(t)$.

Another classical way to obtain orthogonal FMT systems is to use square-root-raised-cosine (SRRC) generators. Indeed, they meet the Nyquist criterion for a $\tilde{T}_0$ time spacing on each subband. What is more, since their frequency occupancy is $[-(1+\alpha)/(2\tilde{T}_0); (1+\alpha)/(2\tilde{T}_0)]$, where α designates the roll-off factor, there is no inter-carrier interference granted that $(1+\alpha)/\tilde{T}_0 \leq \tilde{F}_0$ which is also equivalent to $\alpha \leq 1/\tilde{\rho} - 1$. Finally, we thus obtain tight frames with SRRC generators with roll-off factor $\alpha \leq \rho - 1$. In here, we will use $\alpha = \rho - 1$ and a truncation length equal to $32T_0$.

Finally, we have chosen to also use two types of discrete-time-optimized orthogonal filters published in [20]. The first one is designed in order to minimize out-band energy (OBE), and the second one maximizes time–frequency localization (TFL). They also have the property of having a minimal time duration. With a proper adaption as described previously, they lead to tight frames.

Time and frequency responses of these different filters are depicted in Figs. 5 and 6 for $\rho = 4/3$ and $\rho = 15/16$, respectively, and $M = 128$. It is worthwhile mentioning that when ρ tends toward 1, all ρT_0-duration tight frames tend toward RECT_{T_0}, which explains that time responses of RECT_{T_0}, RECT_{T_0}, and TFL and OBE filters are particularly difficult to distinguish from each other when $\rho = 16/15$ (see Fig. 6).

5 Simulations

5.1 Empirical study of the interference term

In this sub-section, we discuss the relevance of the Gaussian approximation of the interference. To this extent, we measure 3.6×10^6 realizations of the interference term $i_{p,q}$ by performing a transmission of $M = 64$ subcarriers over $K = 50000$ multicarrier symbols for different values of ρ, using a QPSK constellation and tight frames. The variance of the obtained samples is then normalized thus giving standardized versions of $i_{p,q}$ depending on ρ,

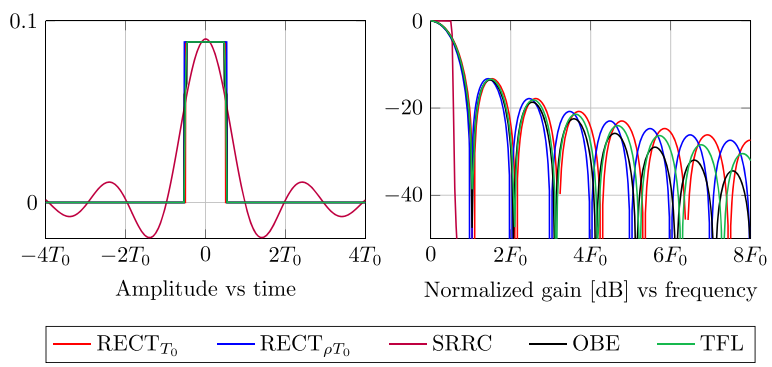

Fig. 6 Generator filters providing dual or tight frames for $\rho = 16/15$

Table 2 χ^2 and Kolmogorov–Smirnov (KS) statistical tests results for the null hypothesis that the real ($\mathcal{R}$) and imaginary part ($\mathcal{I}$) of the interference come from a normal distribution

Pulse shape	ρ	KS rejected		KS p value		χ^2 rejected?		χ^2 p value	
		$\mathcal{R}$	$\mathcal{I}$	$\mathcal{R}$	$\mathcal{I}$	$\mathcal{R}$	$\mathcal{I}$	$\mathcal{R}$	$\mathcal{I}$
TFL	16/15	Yes	Yes	2.1×10^{-6}	2.1×10^{-6}	Yes	Yes	$< 10^{-6}$	$< 10^{-6}$
	8/5	Yes	Yes	$< 10^{-6}$	$< 10^{-6}$	Yes	Yes	$< 10^{-6}$	$< 10^{-6}$
OBE	16/15	Yes	Yes	3.4×10^{-5}	3.4×10^{-5}	Yes	Yes	$< 10^{-6}$	$< 10^{-6}$
	8/5	Yes	Yes	$< 10^{-6}$	$< 10^{-6}$	Yes	Yes	$< 10^{-6}$	$< 10^{-6}$
SRRC	16/15	Yes	Yes	$< 10^{-6}$	$< 10^{-6}$	Yes	Yes	$< 10^{-6}$	$< 10^{-6}$
	8/5	Yes	Yes	$< 10^{-6}$	$< 10^{-6}$	Yes	Yes	$< 10^{-6}$	$< 10^{-6}$
RECT_{T_0}	16/15	Yes	Yes	$< 10^{-6}$	$< 10^{-6}$	Yes	Yes	$< 10^{-6}$	$< 10^{-6}$
	8/5	Yes	Yes	$< 10^{-6}$	$< 10^{-6}$	Yes	Yes	$< 10^{-6}$	$< 10^{-6}$

The rejection criteria are given at 5% confidence level

whose empirical probability density functions and cumulative distribution functions (CDF) are comparable. Thus, we will simply denote by $i|\rho$ the random variable whose realizations are $i_{p,q}$, with the knowledge of ρ. The behavior described here has been observed to be similar for various generators forming tight frames.

We consider a transmission over a noise-free perfect channel ($\text{SINR} = 1/(\rho - 1)$) of zero-mean, independent, and identically distributed symbols. We define two functions $\tilde{F}_{i|\rho}$ and $F_{i|\rho}$ as follows:

$$\tilde{F}_{i|\rho}(x) = \frac{1}{2}\left(\mathrm{P}\left\{\mathcal{R}\{i\} \leq x|\rho\right\} + \mathrm{P}\left\{\mathcal{I}\{i\} \leq x|\rho\right\}\right), \quad (32)$$

where $\mathcal{R}\{\cdot\}$ and $\mathcal{I}\{\cdot\}$ denote the real and imaginary part, respectively, of a complex number, and

$$F_{i|\rho}(x) = \frac{1}{2}\left(\tilde{F}_{i|\rho}(x) + 1 - \tilde{F}_{i|\rho}(-x)\right), \quad (33)$$

such that the bit-error probability can be expressed as:

$$P_e(\rho) = 1 - F_{i|\rho}\left(\sqrt{\text{SINR}}\right) = 1 - F_{i|\rho}\left(\sqrt{\frac{1}{\rho - 1}}\right). \quad (34)$$

As stated in Section 2.2, the central limit theorem does not apply to the interference term. This is confirmed as all statistical tests ran for various prototypes and values of

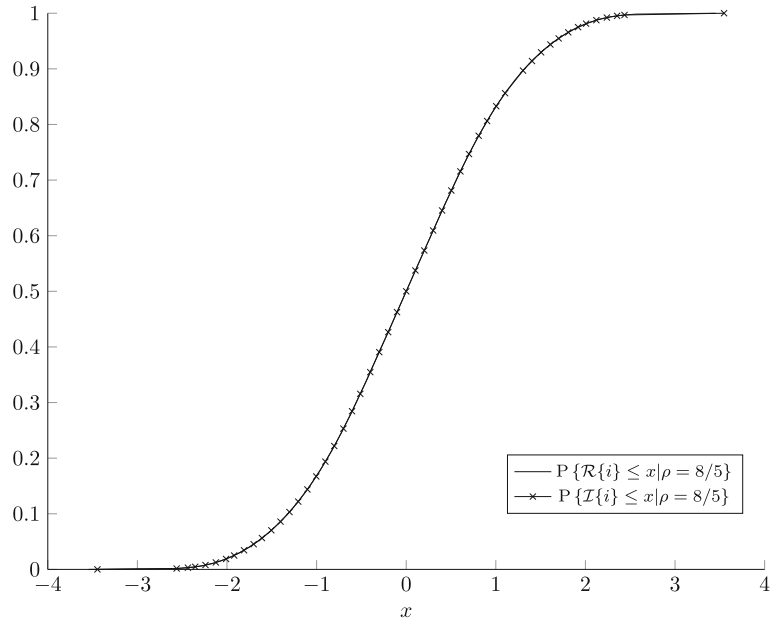

Fig. 7 Example of CDF for real and imaginary part of the interference with $\rho = 8/5$, QPSK constellation. We can see that they are at least very similar and exhibit a rotational symmetry of center (0, 0.5)

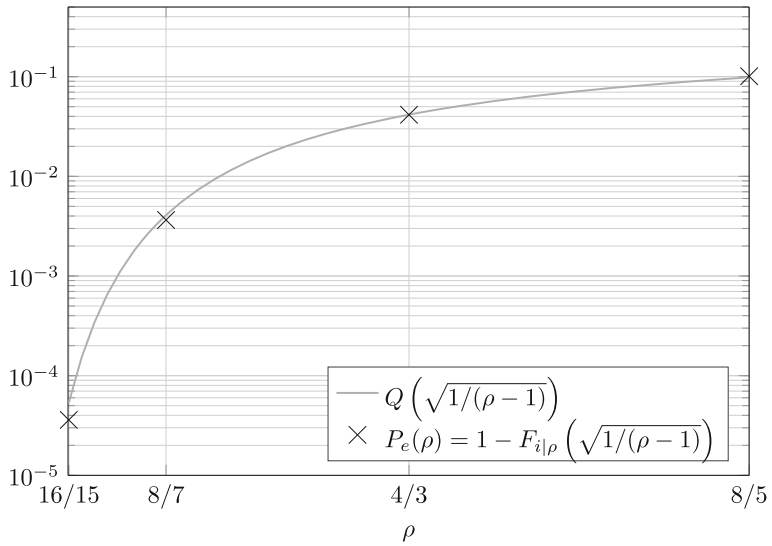

Fig. 8 Comparison of the error probability in absence of noise and its Gaussian approximation depending on ρ, QPSK constellation

ρ rejected the null hypothesis that the real and imaginary part of the interference does come from a normal distribution at the 5% significance level (Table 2). Still, in practice, we notice that $\mathcal{R}\{i|\rho\}$ and $\mathcal{I}\{i|\rho\}$ show identical distribution that furthermore exhibit a central symmetry of center $(0, 0.5)$, as illustrated in Fig. 7. This means that $F_{i|\rho}(x)$ could be replaced by $\mathrm{P}\{\mathcal{R}\{i\} \leq x|\rho\}$ or $\mathrm{P}\{\mathcal{I}\{i\} \leq x|\rho\}$ in the expression of the bit-error probability. However, in absence of any formal proof, this may be a mere simplification.

Since the Gaussian distribution of the interference term is revoked by empirical measurements, one may ask how far the real and Gaussian-approximated bit-error probability are. In order to answer this question, we compare the values of the functions $P_e(\rho)$ and $Q\left(\sqrt{1/(\rho-1)}\right)$ for various ρ in Fig. 8 and conclude that the relative approximation error is negligible, except for ρ which is close to one. Our simulations furthermore revealed that the Gaussian approximation then constitutes an upper bound for the bit-error probability. This result ensures that the

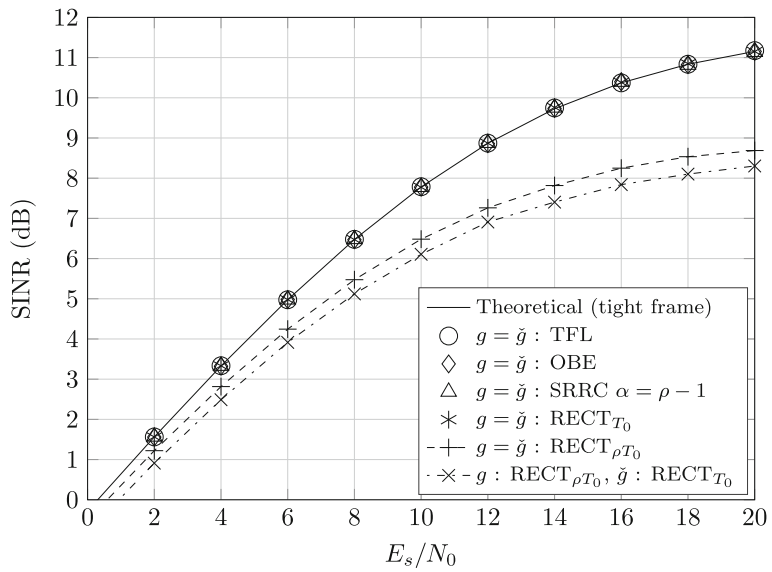

Fig. 9 SINR as a function of E_s/N_0, with $\rho = 16/15$, QPSK constellation

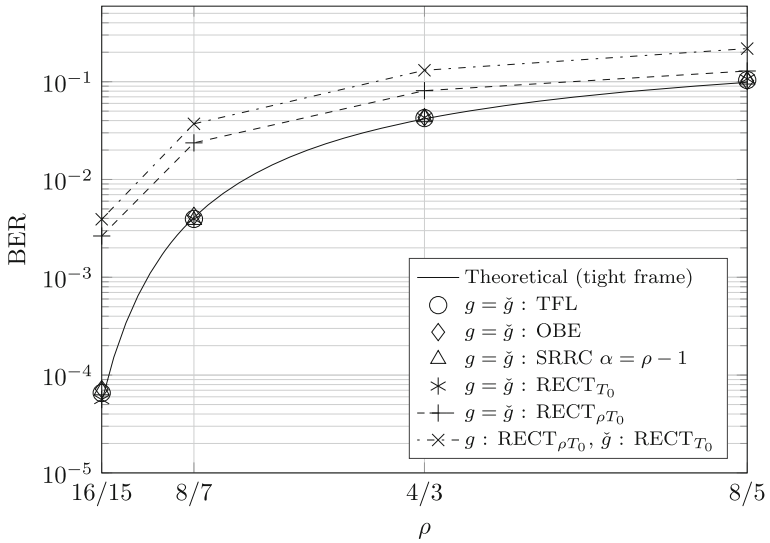

Fig. 10 BER as a function of ρ, with $E_b/N_0 = 20$ dB, QPSK constellation

Gaussian approximation can be safely used for multicarrier FTN communication system design, provided that tight frames are used.

5.2 Linear system performance

The simulations presented in this sub-section consist in the transmission of $K = 5000$ multicarrier symbols over $M = 128$ subcarriers with a QPSK constellation. They were run for various generators, as presented in Section 4.

Figure 9 exhibits the perfect prediction of the SINR by (18) when the generators used in transmission and reception form a dual canonical tight pair of frames. In addition, Figs. 10 and 11 confirm the accuracy of the expression of the bit-error probability (20) and the relevance of the Gaussian approximation of the interference, although we can see its limits for strong E_b/N_0 ($\geq$ 14 dB) and ρ close to 1 ($\rho = 16/15$).

In terms of performance, for this kind of non-coded multicarrier FTN system, Fig. 10 shows that the bit-error rate (BER) rapidly rises with the density. We can also see in Fig. 11 that a lower-bound of the BER appears as noise becomes negligible compared to interference. In addition, and in accordance with the expression of the SINR, the performance gets worse if the frames used are not tight nor canonical dual. These results confirm the needs to develop non-linear detectors allowing for a more efficient IPI mitigation.

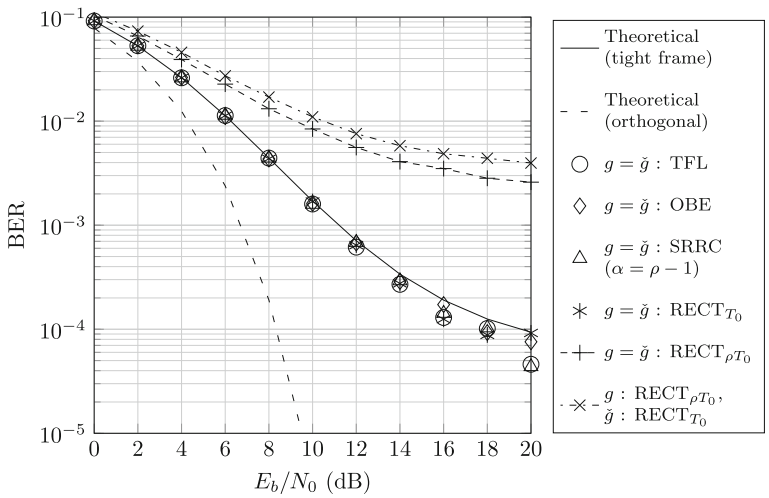

Fig. 11 BER as a function of E_b/N_0, with $\rho = 16/15$, QPSK constellation

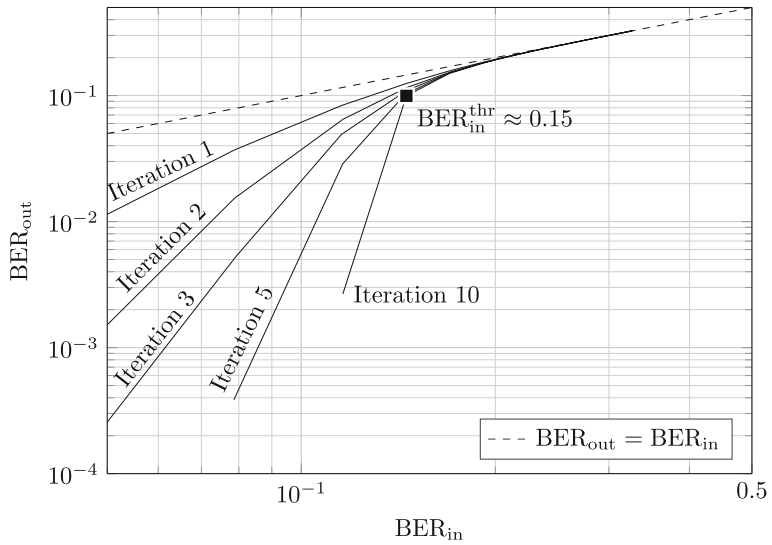

Fig. 12 Output BER ($\mathrm{BER}_{\mathrm{out}}$) as a function of the input BER ($\mathrm{BER}_{\mathrm{in}}$) for a rate 1/2 LDPC encoder/decoder. In this configuration, the convergence threshold is at an input BER of 0.15

5.3 Use in a coded system with iterative decoding

As highlighted in the previous sub-section, a linear system is not sufficient to combine practical BER performance with attractive density gains. To overcome this issue, one can add forward error correction (FEC). In this work, we focus on FEC schemes enabling iterative decoding (e.g., LDPC, turbo codes) due to their good performance at an affordable computational complexity.

Each encoder/decoder can be characterized by its so-called convergence threshold [22]. It is defined as the input BER threshold from which the coded system achieves better performance than the uncoded one. In other words, the convergence threshold is the largest value $\mathrm{BER}_{\mathrm{in}}^{\mathrm{thr}}$ such that $\mathrm{BER}_{\mathrm{out}} < \mathrm{BER}_{\mathrm{in}}$. As an example, Fig. 12 shows that a coded system using the LDPC code of rate 1/2 specified in the DVB-S2 standard [23] has its convergence threshold for an input BER of approximately 0.15. According to (20) in the case of an FTN system using QPSK and tight frames, the SINR at the output of the linear receiver must be such that $Q(\sqrt{\mathrm{SINR}}) < 0.15$ to

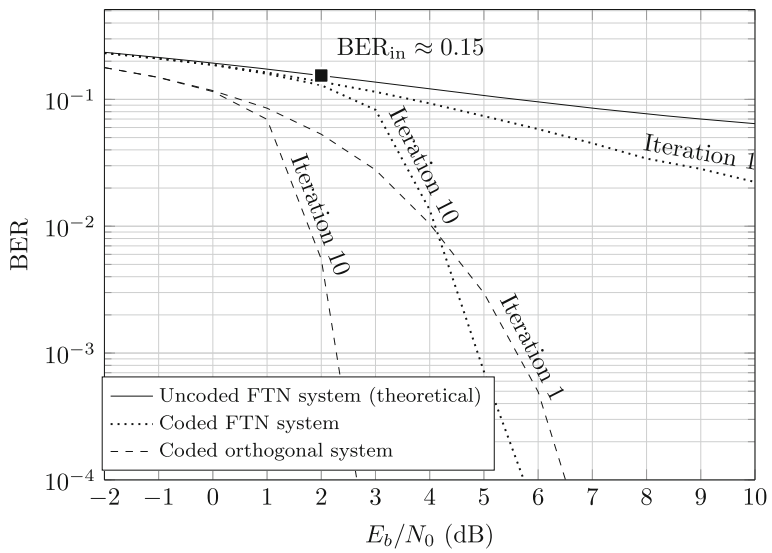

Fig. 13 Comparison of BER versus E_b/N_0 performance, with a TFL generator and a QPSK constellation, of an FTN ($\rho = 4/3$) using a rate 1/2 LDPC code, and an orthogonal system ($\rho = 1$) using a rate 2/3 LDPC code for ten iterations of the decoders. Both systems have the same spectral efficiency $\eta = 4/3$ bits/s/Hz

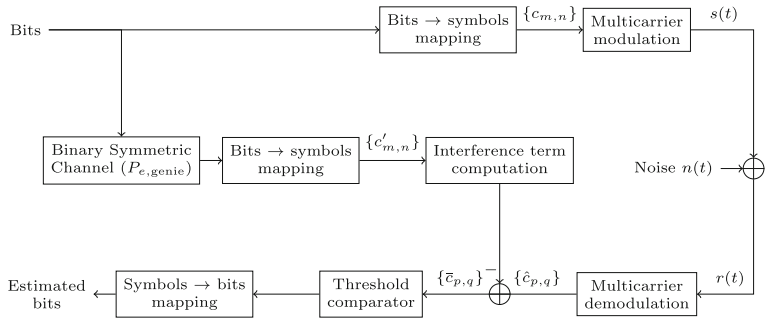

Fig. 14 Block diagram of the pseudo-genie interference cancellation receiver

yield convergence of the decoder. These constraints can easily be fulfilled by setting appropriate restrictions to E_b/N_0 and ρ.

In Fig. 13, we observe that when used with a multicarrier FTN system using tight frames, the coded system converges as expected when the input BER goes below 0.15, at $E_b/N_0 = 2$ dB. However, we can see in Fig. 13 that this FTN system is surpassed by the orthogonal one using the rate 2/3 LDPC code of the DVB-S2 standard, which provides the same spectral efficiency. This advocates for dedicated strategies of interference mitigation in FTN systems, as treating it as noise does not allow for a full use of the available knowledge on the self-interference structure.

5.4 Performance with interference cancellation

From the expressions of the bit-error probabilities (20) (21), it is obvious that the FTN linear system shows worse performance compared to the orthogonal case. Besides, from the expression of the received signal (8), one can notice that the performance of the orthogonal system can be retrieved by removing the interference induced by the FTN system, allowing for an improvement of the spectral efficiency of the transmission while keeping the same BER.

Such an interference cancellation (IC) is usually performed by estimating the received symbols, then computing the interference term from these estimations and subtract it to the received signal. Given that this estimation might not be perfect, it is interesting to assess the behavior of this system in presence of errors on the estimated symbols. To fulfill that purpose, we implemented the pseudo-genie receiver depicted by Fig. 14. The difference with a "true genie" receiver is that its knowledge of the transmitted symbols is corrupted by a binary symmetric channel inducing an error probability $P_{e,\text{genie}}$ on the bits used to compute the interference term.

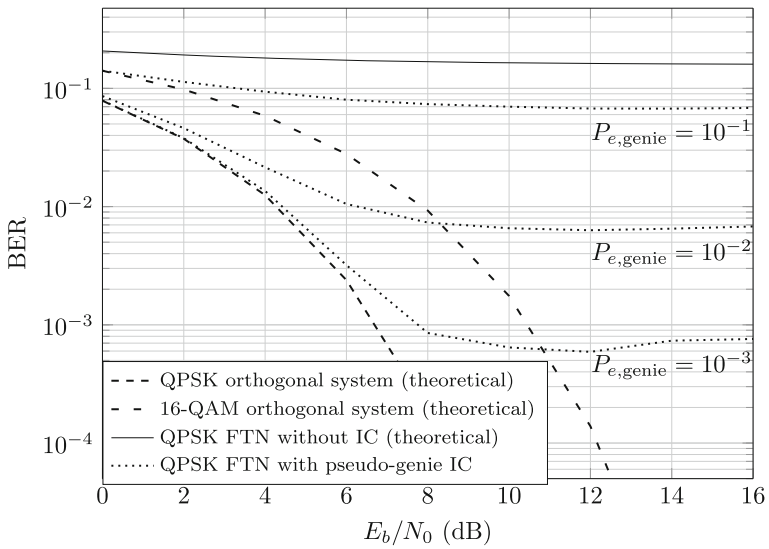

Fig. 15 BER as a function of E_b/N_0, with a pseudo-genie receiver, $\rho = 2$, a TFL generator, and $P_{e,\text{genie}} \in \{10^{-1}, 10^{-2}, 10^{-3}\}$ compared to an orthogonal ($\rho = 1$) 16-QAM transmission (both schemes have a spectral efficiency $\eta = 4$ bits/s/Hz)

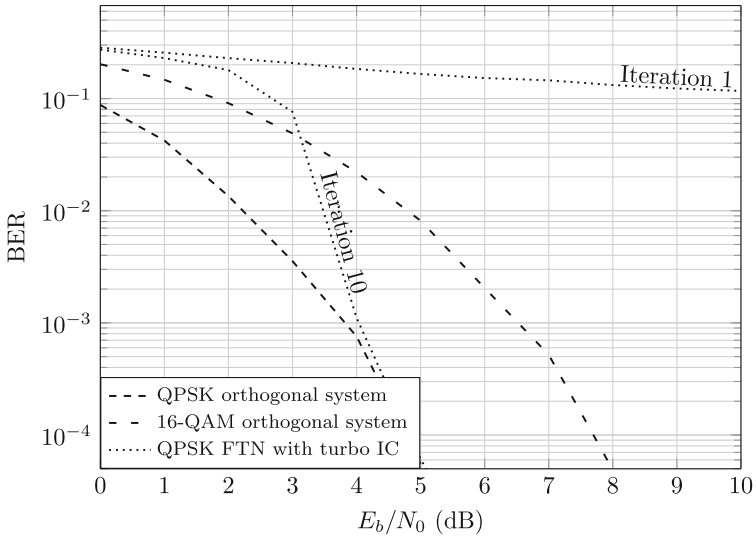

Fig. 16 BER as a function of E_b/N_0, with a turbo IC receiver (10 iterations), $\rho = 2$ and a TFL generator were compared to an orthogonal ($\rho = 1$) 16-QAM transmission, both coded with a (7, 5) convolutional code (spectral efficiency $\eta = 2$ bits/s/Hz)

Figure 15 presents the performance of this system with a density $\rho = 2$ and a QPSK constellation, compared to an orthogonal system using a 16-QAM constellation. In these simulations, $K = 5000$ multicarrier symbols were transmitted over $M = 32$ subcarriers using a TFL generator. Firstly, we can see that this FTN system with interference cancellation is quite robust to errors on the bits used to compute and cancel the interference. This gives an insight on how non-linear receivers using interference cancellation (such as decision feedback or turbo equalization) could efficiently prevent inter-carrier interference. Secondly, we notice that at low SNR, this system can rapidly surpass the 16-QAM orthogonal system having the same spectral efficiency as the probability of error on the estimated bits gets lower. However, two facts ask for a refinement of this technique: (i) the BER of the linear receiver is too high to allow for a good interference cancellation in, for instance, a simple decision–feedback setup and (ii) even with a low error probability; one can observe an error floor at high SNR.

A viable option to circumvent these two limitations is to associate the IC with an error-correcting code with probabilistic information exchange between the two, that is, using a "turbo" structure ([22], Chap. 11). Indeed, using an error-correcting code should lower the bit-error rate at the first iteration. Also, using "soft symbols" should avoid pollution of the interference cancellation by unreliable symbols. Simulation of Fig. 16 uses a convolutional code with polynomial $(7, 5)_8$ (rate $R = 1/2$), decoded with a SISO BCJR decoder [24]. The soft symbols used by the IC, as well as its output log likelihood ratios, are computed following the conventions established by previous works on linear turbo equalization [25]. The other parameters are the following: the encoder is fed with $N_b = 16,384$ bits, and the coded bits on its output are shuffled with an interleaver and given to a binary to symbols converter (using QPSK or 16-QAM) and then to the multicarrier modulator using $M = 32$ subcarriers. This setup allows for a fair comparison of the orthogonal 16-QAM and the FTN ($\rho = 2$) QPSK coded systems as they have same spectral efficiency $\eta = 2$. Here, we observe that indeed, using turbo IC allows better BER performance than orthogonal 16-QAM for $E_b/N_0 > 3.1$ and does not suffer from the problem of error floor at high SNR.

6 Conclusions

Through this article, we specified a linear multicarrier system based on the use of overcomplete Gabor frames, enabling an increase in signaling density in the time and/or the frequency domain and leading to a bidimensional FTN system. Consequently, an increase of the spectral efficiency beyond (bi)-orthogonal systems (for a given constellation size) yields interference between pulse shapes.

The results presented in this article compare the performance of FTN multicarrier systems based on the parameters of their linear stage (e.g., time–frequency lattice density, transmission/reception generators...) in the presence of additive white Gaussian noise. Additionally, guidelines for efficiently choosing transmission/reception generators and implementing the discrete-time equivalent linear system are provided.

Finally, we have shown that the performance of linear systems should be studied before designing more complex receiver structures (e.g., LDPC/turbo decoders, turbo equalizers). Besides, such a separate analysis helps to lower simulations' computational complexity.

Future work includes the assessment of the complete FTN multicarrier system over more realistic channel models (e.g., fading...). More precisely, it would be interesting to evaluate the robustness of such a system in the presence of an imperfect channel estimation.

Acknowledgements
The authors would like to address a particular thanks to Dr. Laurent Ros for his valuable advices and relevant remarks concerning this work.

Authors' contributions
This article is an extended version of AM, CS, DR, and PS' "Analysis of a Multicarrier Communication System Based on Overcomplete Gabor Frames," Cognitive Radio Oriented Wireless Networks, Springer International Publishing, p.387, 2016, *Lecture Notes of the Institute for Computer Sciences, Social Informatics and Telecommunications Engineering*, 978-3-319-40352-6. All authors read and approved the final manuscript.

Competing interests
The authors declare that they have no competing interests.

Publisher's Note

Springer Nature remains neutral with regard to jurisdictional claims in published maps and institutional affiliations.

Author details
[1]Univ. Grenoble Alpes, GIPSA-Lab, F-38400 Grenoble, France. [2]Institut Supérieur de l'Aéronautique et de l'Espace (ISAE-SUPAERO), Univ. Toulouse, F-31055 Toulouse, France. [3]Independent Researcher, F-35200 Rennes, France.

Received: 28 October 2016 Accepted: 5 May 2017
Published online: 30 May 2017

References

1. H Nyquist, Certain topics in telegraph transmission theory. Trans. Am. Inst. Electr. Eng. **47**(2), 617–644 (1928)
2. GD Forney, Maximum-likelihood sequence estimation of digital sequences in the presence of intersymbol interference. IEEE Trans. Inf. Theory. **18**(3), 363–378 (1972)
3. JE Mazo, Faster than Nyquist signaling. Bell Syst. Tech. J. **54**, 1451–1462 (1975)
4. F Rusek, JB Anderson, in *Proceedings of the International Symposium on Information Theory, ISIT 2005*. The two dimensional Mazo limit (IEEE, Adelaide, 2005), pp. 970–974
5. O Christensen, *Frames and bases: an introductory course*. (Birkhäuser Basel, Boston, 2008)
6. FM Han, XD Zhang, Wireless multicarrier digital transmission via Weyl–Heisenberg frames over time-frequency dispersive channels. IEEE Trans. Commun. **57**(6), 1721–1733 (2009)
7. FM Han, XD Zhang, Asymptotic equivalence of two multicarrier transmission schemes in terms of robustness against time-frequency dispersive channels. IEEE Trans. Veh. Technol. **59**(2), 682–691 (2010)
8. F Rusek, JB Anderson, in *Proceedings of the International Symposium on Information Theory, ISIT 2006*. Serial and parallel concatenations based on faster than Nyquist signaling (IEEE, Seattle, 2006), pp. 1993–1997
9. D Dasalukunte, F Rusek, V Owall, Multicarrier faster-than-Nyquist transceivers: hardware architecture and performance analysis. IEEE Trans. Circ. Syst. I Regular Papers. **58**(4), 827–838 (2011)
10. C Siclet, D Roque, H Shu, P Siohan, in *11th International Symposium on Wireless Communications Systems, ISWCS 2014*. On the study of faster-than-Nyquist multicarrier signaling based on frame theory (IEEE, Barcelona, 2014), pp. 251–255
11. I Daubechies, The wavelet transform, time-frequency localization and signal analysis. IEEE Trans. Inf. Theory. **36**(5), 961–1005 (1990)
12. JG Proakis, M Salehi, *Digital communications*, McGraw-Hill International Edition. (McGraw-Hill, 2008). https://books.google.fr/books?id=ksh0GgAACAAJ
13. K Cho, D Yoon, On the general BER expression of one- and two-dimensional amplitude modulations. IEEE Trans. Commun. **50**(7), 1074–1080 (2002)
14. D Roque, C Siclet, Performances of weighted cyclic prefix OFDM with low-complexity equalization. IEEE Commun. Lett. **17**(3), 439–442 (2013). Available at https://hal.archives-ouvertes.fr/hal-01260517
15. JW Cooley, JW Tukey, An algorithm for the machine calculation of complex Fourier series. Math. Comput. **19**(90), 297–301 (1965)
16. L Rabiner, R Schafer, C Rader, The chirp z-transform algorithm. IEEE Trans. Audio Electroacoustics. **17**(2), 86–92 (1969)
17. G Cherubini, E Eleftheriou, S Olcer, Filtered multitone modulation for very high-speed digital subscriber lines. IEEE J. Sel. Areas Commun. **20**(5), 1016–1028 (2002)
18. C Siclet, P Siohan, D Pinchon, in *Proceedings of the 14th International Conference on Digital Signal Processing, DSP 2002*. Oversampled orthogonal and biorthogonal multicarrier modulations with perfect reconstruction, vol. 2 (IEEE, Santorini, 2002), pp. 647–650
19. AM Tonello, in *Proceedings of the International Conference on Acoustics, Speech and Signal Processing, ICASSP 2006*. Time domain and frequency domain implementations of FMT modulation architectures, vol. 4 (IEEE, Toulouse, 2006)
20. D Pinchon, P Siohan, in *Proceedings of the Global Telecommunications Conference, GLOBECOM 2011*. Closed-form expressions of optimal short PR FMT prototype filters (IEEE, Houston, 2011)
21. C Siclet, P Siohan, D Pinchon, Perfect reconstruction conditions and design of oversampled DFT-modulated transmultiplexers. EURASIP J. Appl. Signal Process. **2006**, 1–14 (2006)
22. C Berrou, K Amis Cavalec, M Arzel, A Glavieux, M Jezequel, C Langlais, R Le Bidan, S Saoudi, G Battail, E Boutillon, Y Saouter, E Maury, C Laot, S Kerouedan, F Guilloud, C Douillard, *Codes et Turbocodes Iris*. (Springer, Paris, 2007)
23. S Morosi, R Fantacci, ED Re, R Suffritti, in *Satellite Communications and Navigation Systems. Signals and Communication Technology*, ed. by ED Re, M Ruggieri. Iterative Demapping and Decoding for DVB-S2 Communications (Springer, Boston, 2008)
24. L Bahl, J Cocke, F Jelinek, J Raviv, Optimal decoding of linear codes for minimizing symbol error rate (corresp). IEEE Trans. Inf. Theory. **20**(2), 284–287 (1974)
25. C Laot, R Le Bidan, D Leroux, Low-complexity MMSE turbo equalization: a possible solution for EDGE. IEEE Trans. Wirel. Commun. **4**(3), 965–974 (2005)

Submit your manuscript to a SpringerOpen journal and benefit from:

- ► Convenient online submission
- ► Rigorous peer review
- ► Immediate publication on acceptance
- ► Open access: articles freely available online
- ► High visibility within the field
- ► Retaining the copyright to your article

Submit your next manuscript at ► springeropen.com